

Strong-coupling theory of the upper critical magnetic field H_{c2}

M. Schossmann

Physics Department, MacMaster University, Hamilton, Ontario, L8S 4M1 Canada

E. Schachinger

Institut für Theoretische Physik, Technische Universität Graz, A-8010 Graz, Austria

(Received 16 October 1985; revised manuscript received 6 January 1986)

In this paper a strong-coupling theory of the upper critical magnetic field (H_{c2}) is developed within the framework of the Werthamer-Helfand-Hohenberg theory. We include Pauli paramagnetic limiting and momentum scattering of the conduction electrons at randomly distributed impurity sites. The developed theory is tested against experimental data available for niobium and V_3Si . It is shown that for isotropic cases the presented theory gives excellent agreement with experiment over the complete temperature range. It is remarkable that it was not necessary in both cases to include spin-orbit scattering. It can be concluded that in most cases spin-orbit scattering was only used to compensate for strong-coupling effects in the older Bardeen-Cooper-Schrieffer—related theories.

I. INTRODUCTION

The first theoretical descriptions of the upper critical magnetic field (H_{c2}) were based on the Ginzburg-Landau-Abrikosov-Gor'kov¹⁻³ (GLAG) theory and were applicable to practically all superconductors. On the other hand, these theories were restricted to temperatures T close to the critical temperature T_c of the specific superconductor. Maki⁴ and de Gennes⁵ later independently calculated the full temperature dependence for H_{c2} in the dirty (small-mean-free-path) limit. It was then the main contribution of Werthamer and co-workers⁶⁻⁸ (WHH theory) to develop a set of equations which described the critical field at the second-order transition, where the superconductor gap function $\Delta(r)$ is vanishing. The resulting description was valid for the whole temperature range and included momentum scattering at impurity sites, Pauli spin paramagnetism, and electron spin-orbit scattering.

All these theoretical descriptions were based on the Bardeen-Cooper-Schrieffer (BCS) theory of superconductivity, and the application of these theories to specific experimental data very often revealed that the experimental data were almost perfectly reproduced at high temperatures, while in the low-temperature range the theory usually predicted smaller values for H_{c2} than were experimentally observed. Werthamer and McMillan⁹ included the full electron-phonon interaction, in the way suggested by Eliashberg,¹⁰ in order to overcome the apparent failure of the BCS-based theory in the low-temperature region of the H_{c2} results for the transition-material niobium. They developed equations on the real axis and concluded from their results for niobium that strong-coupling effects seem not to be important, at least not in explaining the physical behavior of niobium. They claimed that anisotropy seems to be the explanation of the observed deviation of the experimental data from the theoretical predictions.

Later, further strong-coupling formulations were presented by Eilenberger and Ambegaokar,¹¹ Usadel,¹² Rainer and Bergman,¹³ and Rainer *et al.*¹⁴ All these for-

mulations were based on the "dirty limit," where the resulting equations become especially simple. Recently, Schossmann and Schachinger¹⁵ extended this strong-coupling theory to the case of superconductors with non-constant electronic density of states at the Fermi surface in an attempt to give a better explanation of the situation which may be relevant to $A15$ superconductors.

Orlando *et al.*¹⁶ realized, in their thorough analysis of the experimental results of the upper critical field in the $A15$ compounds V_3Si and Nb_3Sn , that it was necessary to include the normal-state renormalization of the electronic frequencies in the form $\tilde{\omega}_n = \omega_n(1 + \lambda)$ in order to achieve a satisfying theoretical description of the experimental data. (λ is the mass-enhancement factor due to electron-phonon interaction.) They observed that Pauli paramagnetic limiting was essential to explain the behavior of V_3Si , and they had to include substantial spin-orbit scattering in order to get a satisfying theoretical description of the low-temperature data.

In the meanwhile it became obvious that strong coupling not only results in quantitative deviations from BCS predictions, but also in qualitative ones, whenever magnetic effects in superconductors are investigated.¹⁷⁻¹⁹ It therefore seemed to be justified to make a second attempt to include the full electron-phonon interaction with the WHH theory of H_{c2} . In his thesis Schossmann²⁰ derived the necessary equations on the imaginary axis and these equations were used by Schachinger *et al.*^{21,22} in their simplest form to calculate H_{c2} for the Chevrel compound $Cu_2Mo_6S_8$. It was possible to prove that the strong-coupling calculation of the WHH theory resulted in much better agreement with experiment, especially in the region at low temperatures.

In this paper we want to develop the strong-coupling theory of the upper critical magnetic field including Pauli paramagnetic limiting and electron-momentum scattering at randomly distributed impurities. The outline of the paper is as follows: In Sec. II we present the main theoretical points necessary to derive strong-coupling equations

for H_{c2} on the imaginary axis. As we follow very closely the WHH theory, we concentrate on the problem of how to include the full electron-phonon interaction. In Sec. III we compare theoretical predictions of our formulas with experimental data recently found for niobium and the V_3Si data reported by Foner and McNiff.²³ Finally, in Sec. IV, conclusions are drawn.

II. THEORY

The full thermodynamic electron Green's function is determined by perturbation series:

$$G = G_0 + G_0 \cdot \sum_{n=1}^{\infty} (\Sigma \cdot G_0)^n, \quad (1)$$

where $x \cdot y$ is a convolution integral if Eq. (1) is evaluated in local space and a simple product if (1) is evaluated in Fourier space. G_0 is the electron Green's function of the unperturbed system and Σ is the full electron self-energy. In the case of a superconductor, G_0 , G , and Σ are 4×4 matrices, in agreement with Nambu's formalism.²⁴ Thus we can split G into two matrices, one of which is diagonal and represents the normal-state properties of the system under consideration. The second matrix is purely off diagonal and describes the superconducting state:

$$G = \begin{pmatrix} G_1 & 0 & 0 & 0 \\ 0 & G_2 & 0 & 0 \\ 0 & 0 & G_3 & 0 \\ 0 & 0 & 0 & G_4 \end{pmatrix} + \begin{pmatrix} 0 & 0 & 0 & \Phi_1 \\ 0 & 0 & \Phi_2 & 0 \\ 0 & \Phi_3 & 0 & 0 \\ \Phi_4 & 0 & 0 & 0 \end{pmatrix} \\ = G_d + G_{\text{off}}. \quad (2)$$

The total self-energy may be decomposed in the same way:

$$\Sigma = \Sigma_d + \Sigma_{\text{off}}. \quad (3)$$

We apply (2) and (3) to (1) and find, for the normal state,

$$G_n = G_d = G_0 + G_0 \cdot \sum_{n=1}^{\infty} (\Sigma_d \cdot G_0)^n, \quad (4)$$

and, for the off-diagonal part of the Green's function,

$$G_{\text{off}} = G_n \cdot \Sigma_{\text{off}} \cdot G_n. \quad (5)$$

It is now essential to calculate the normal-state Green's function in its local-space representation. The starting

point is the equation of motion of a system in a magnetic field \mathbf{H} (μ is the chemical potential):

$$\left[\frac{\partial}{\partial \tau} - \frac{1}{2m} \left(\frac{\nabla}{i} - \frac{e}{c} \mathbf{A}(\mathbf{x}) \right)^2 - \mu - \frac{e}{m} \boldsymbol{\sigma} \cdot \mathbf{H} \right] G_{n0}(\mathbf{x}, \mathbf{x}'; \tau, \tau') \\ = \delta(\mathbf{x} - \mathbf{x}') \delta(\tau - \tau'), \quad (6)$$

which can be solved applying the rules developed by Werthamer *et al.*⁸ (WHH). According to their calculations, the influence of the vector potential $\mathbf{A}(\mathbf{x})$ results in a phase factor by which the Green's function for $\mathbf{H}=0$ is multiplied:

$$G_n(\mathbf{x}, \mathbf{x}'; \tau, \tau') = G_n(\mathbf{x}, \mathbf{x}'; \tau, \tau') |_{H=0} \\ \times \exp \left[-\frac{ie}{c} \int_{\mathbf{x}}^{\mathbf{x}'} d\mathbf{s} \cdot \mathbf{A}(\mathbf{s}) \right]. \quad (7)$$

It was shown by WHH that this rule can even be applied to a Green's function G_{n0} calculated from Eq. (6) with $\mathbf{A}(\mathbf{x})$ set equal to zero. In this case Eq. (6) can be transformed into Fourier space and we find

$$G_{n0}(\epsilon_{\mathbf{k}}, i\omega_n)^{-1} = i\omega_n \tau_0 \cdot \sigma_0 - \epsilon \tau_3 \cdot \sigma_0 - (e/m) H \tau_3 \cdot \sigma_3, \quad (8)$$

with ω_n the Matsubara frequencies $\pi T(2n+1)$, $n=0, \pm 1, \pm 2, \dots$, $\epsilon_{\mathbf{k}}$ the electronic states of the unperturbed system, and $\tau_i \cdot \sigma_j$ ($i, j=0, 1, 2, 3$) the direct product of two Pauli matrices. (The index 0 indicates a 2×2 unit matrix.) The magnetic field \mathbf{H} was assumed to be parallel to the z axis. Equation (4) is easily solved using the ansatz

$$G(\epsilon, i\omega_n)^{-1} = i\tilde{\omega}_n \tau_0 \cdot \sigma_0 - \epsilon \tau_3 \cdot \sigma_0 - \chi \tau_0 \cdot \sigma_3 - b \tau_3 \cdot \sigma_3, \quad (9)$$

and by introducing the standard expression for the electron-phonon interaction,

$$\Sigma_{e\text{-ph}}(\epsilon, i\omega_n) = T \sum_{\omega_m} \lambda(\omega_m) \int_{-\infty}^{\infty} d\epsilon' G(\epsilon'; i\omega_n - i\omega_m), \quad (10)$$

with

$$\lambda(\omega_n) = 2 \int_0^{\infty} d\Omega \frac{\Omega}{\Omega^2 + \omega_n^2} \alpha(\Omega)^2 F(\Omega), \quad (11)$$

and $\alpha(\Omega)^2 F(\Omega)$ is the electron-phonon interaction spectral density. The electron-impurity interaction for randomly distributed impurity sites is according to Abrikosov and Gor'kov²⁵ described by the self energy contribution:

$$\Sigma_I(\mathbf{k}, i\omega_n) = \int d^3q V(\mathbf{q}) G(\mathbf{k}-\mathbf{q}, i\omega_n) V(-\mathbf{q}) \approx i\pi t_+ \text{sgn}(\tilde{\omega}_n) \tau_0 \cdot \sigma_0, \quad t_+ = 1/(2\pi\tau_{\text{tr}}) \quad (12)$$

where we introduced the transport relaxation time τ_{tr} :

$$\frac{1}{\tau_{\text{tr}}} = 2\pi n_I N(0) \int \frac{d\Omega'}{4\pi} |V(k_F, \theta)|^2, \quad (13)$$

with the Fermi momentum k_F , the impurity concentration n_I , the density of states at the Fermi surface $N(0)$, and the angle θ between the incoming and outgoing electron momentum.

Solving Eq. (4), we find

$$\tilde{\omega}_n = \omega_n + \pi T \sum_{m=-\infty}^{\infty} \lambda(\omega_n - \omega_m) \text{sgn}(\tilde{\omega}_m) + \frac{1}{2\tau_{\text{tr}}} \text{sgn}(\tilde{\omega}_n), \quad (14a)$$

$$\epsilon = \epsilon_{\mathbf{k}}, \quad \chi = 0, \quad b = (e/m)H. \quad (14b)$$

χ is equal to zero because the electronic density of states is assumed to be symmetrical with respect to the Fermi surface.

We are now in a position to calculate the local-space representation of the components $G_{1,4}$ of the full normal-state Green's function:

$$G_{1,2}(\mathbf{x}, \mathbf{x}', i\omega_n) = -\frac{k_F}{2\pi v_F |\mathbf{x} - \mathbf{x}'|} \exp \left\{ \left[i \left[k_F \mp \frac{eH}{v_F m} \right] \text{sgn}(\tilde{\omega}_n) - \frac{\tilde{\omega}_n}{v_F} \right] |\mathbf{x} - \mathbf{x}'| - \frac{ie}{c} \int_{\mathbf{x}}^{\mathbf{x}'} d\mathbf{s} \mathbf{A}(\mathbf{s}) \right\}, \quad (15a)$$

with v_F the Fermi velocity calculated from the isotropic Fermi-gas picture and

$$G_{3,4}(\mathbf{x}, \mathbf{x}', i\omega_n) = -[G_{1,2}(\mathbf{x}, \mathbf{x}', i\omega_n)]^*, \quad (15b)$$

where the upper sign in Eq. (15a) belongs to G_1 . The off-diagonal part of the Green's function G is determined by Eqs. (2) and (5):

$$\begin{pmatrix} 0 & 0 & 0 & \Phi_1 \\ 0 & 0 & \Phi_2 & 0 \\ 0 & \Phi_3 & 0 & 0 \\ \Phi_4 & 0 & 0 & 0 \end{pmatrix} = - \begin{pmatrix} 0 & 0 & 0 & G_1 \cdot \Sigma_{o1} \cdot G_2^* \\ 0 & 0 & G_2 \cdot \Sigma_{o2} \cdot G_1^* & 0 \\ 0 & G_1^* \cdot \Sigma_{o3} \cdot G_2 & 0 & 0 \\ G_2^* \cdot \Sigma_{o4} \cdot G_1 & 0 & 0 & 0 \end{pmatrix}, \quad (16)$$

where Σ_{o1-4} denote the off-diagonal elements of the 4×4 total self-energy matrix. It was already pointed out by Werthamer and McMillan⁹ that the interactions significant for superconductivity are of very short range in local space. It is therefore a good approximation to assume the self-energy contribution of the form

$$\Sigma(\mathbf{x}, \mathbf{x}', i\omega_n) = \Sigma(\mathbf{x}, i\omega_n) \delta(\mathbf{x} - \mathbf{x}'). \quad (17)$$

From the general structure of the self-energy and because of the result (15), it becomes obvious that $\Sigma_{o3,4} = (\Sigma_{o1,2})^*$ and $\Phi_{3,4} = (\Phi_{1,2})^*$. Therefore we can concentrate on the evaluation of the two matrix elements $\Phi_{1,2}$:

$$\begin{aligned} \Phi_{1,2}(\mathbf{x}, i\omega_n) &= \int d^3y G_{1,2}(\mathbf{x}, \mathbf{y}, i\omega_n) \Sigma_{o1,2}(\mathbf{y}, i\omega_n) G_{2,1}(\mathbf{y}, \mathbf{x}, i\omega_n)^* \\ &= - \left[\frac{k_F}{2\pi v_F} \right]^2 \int \frac{d^3y}{|\mathbf{x} - \mathbf{y}|^2} \Sigma_{o1,2}(\mathbf{y}, i\omega_n) \exp \left[-\frac{2}{v_F} \left[\tilde{\omega}_n \pm \frac{ieH}{m} \text{sgn}(\tilde{\omega}_n) \right] |\mathbf{x} - \mathbf{y}| - 2\frac{ie}{c} \int_{\mathbf{x}}^{\mathbf{y}} d\mathbf{s} \mathbf{A}(\mathbf{s}) \right]. \end{aligned} \quad (18)$$

Using the explicit form of the local-space representation of the self-energy matrix element $\Sigma_{o1,2}$ and introducing the Coulomb pseudopotential μ^* in the standard form,²⁶ we arrive at the following equations:

$$\Phi_{1,2}(\mathbf{x}, i\omega_n) = \frac{T}{N(0)} \sum_m [\lambda(\omega_n - \omega_m) - \mu^*] O_{1,2} \Phi_{1,2}(\mathbf{y}, i\omega_m) + \frac{\pi t_+}{N(0)} O_{1,2} \Phi_{1,2}(\mathbf{x}, i\omega_n), \quad (19)$$

where we introduced the integral operator

$$O_{1,2} = \left[\frac{k_F}{2\pi v_F} \right]^2 \int \frac{d^3y}{|\mathbf{x} - \mathbf{y}|^2} \exp \left[-\frac{2}{v_F} \left[\tilde{\omega}_n \pm \frac{ieH}{m} \text{sgn}(\tilde{\omega}_n) \right] |\mathbf{x} - \mathbf{y}| - 2\frac{ie}{c} \int_{\mathbf{x}}^{\mathbf{y}} d\mathbf{s} \mathbf{A}(\mathbf{s}) \right]. \quad (20)$$

The terms in Eq. (19) are of the form

$$\int \frac{d^3y}{|\mathbf{x} - \mathbf{y}|^2} \exp \left[-\beta |\mathbf{x} - \mathbf{y}| - 2\frac{ie}{c} \int_{\mathbf{x}}^{\mathbf{y}} d\mathbf{s} \mathbf{A}(\mathbf{s}) \right] f(\mathbf{y}) = \int \frac{d^3r}{r^2} \exp \left[-\beta |\mathbf{r}| - \mathbf{r} \left[\nabla - \frac{2ie}{c} \mathbf{A}(\mathbf{r}) \right] \right] f(\mathbf{x}), \quad (21)$$

as was shown by Helfand and Werthamer.⁷ Equation (19) clearly allows separation of variables:

$$\Phi_{1,2}(\mathbf{x}, i\omega_n) = \tilde{\Delta}_{1,2}(i\omega_n) f_{1,2}(\mathbf{x}), \quad (22)$$

where the $f_{1,2}(\mathbf{x})$ are the solutions of equations

$$\chi_{1,2}(\tilde{\omega}_n) f_{1,2}(\mathbf{x}) = O_{1,2} f_{1,2}(\mathbf{x}), \quad (23)$$

where the $\chi_{1,2}(\tilde{\omega}_n)$ are the eigenvalues of the operators $O_{1,2}$. The result (21) allows one to transform the integral equations (19) into differential equations of infinite order, from which we can determine the eigenvalues $\chi_{1,2}(\tilde{\omega}_n)$.

As we are only interested in the upper critical field of the system, we have to keep only the smallest eigenvalues:

$$\frac{\chi_{1,2}(\tilde{\omega}_n)}{N(0)\pi} = \frac{2}{\sqrt{\alpha}} \int_0^\infty dq \exp(-q^2) \times \tan^{-1} \left[\frac{q\sqrt{\alpha}}{|\tilde{\omega}_n| \pm ieH \operatorname{sgn}(\tilde{\omega}_n)/m} \right], \quad (24)$$

with

$$\alpha = eH_{c2}(T)v_F^2. \quad (25)$$

We finally arrive at two equations for the frequency part of the off-diagonal Green's function:

$$\tilde{\Delta}_{1,2}(i\omega_n) = \pi T \sum_{\omega_c} [\lambda(\omega_n - \omega_m) - \mu^*] \chi_{1,2}(\omega_m) \tilde{\Delta}_{1,2}(i\omega_m) + \pi t_+ \chi_{1,2}(\tilde{\omega}_n) \tilde{\Delta}_{1,2}(i\omega_n), \quad (26)$$

with ω_c the cutoff frequency usually chosen to be an integer multiple of the Debye frequency. Obviously $\chi_2(i\omega_n) = [\chi_1(i\omega_n)]^*$ and Eqs. (26) allow two possible choices for the gap function, (i) $\tilde{\Delta}_2 = \tilde{\Delta}_1^*$ or (ii) $\tilde{\Delta}_2 = -\tilde{\Delta}_1^*$, and we make use of one of the two equations (26) to calculate the complex function $\tilde{\Delta}_1(i\omega_n)$. We define

$$\tilde{\Delta}(i\omega_n) = \tilde{\Delta}(i\omega_n) = \tilde{\Delta}_r(i\omega_n) + i\tilde{\Delta}_i(i\omega_n), \quad (27a)$$

$$\chi_1(\tilde{\omega}_n) = \chi(\tilde{\omega}_n) = \chi_r(\tilde{\omega}_n) + i\chi_i(\tilde{\omega}_n). \quad (27b)$$

The solution is

$$\tilde{\Delta}_r(i\omega_n) = \pi T \sum_m [\lambda(\omega_n - \omega_m) - \mu^*] \times [\chi_r(\tilde{\omega}_m) \tilde{\Delta}_r(i\omega_m) - \chi_i(\omega_m) \tilde{\Delta}_i(i\omega_m)] + \pi t_+ [\chi_r(\tilde{\omega}_n) \tilde{\Delta}_r(i\omega_n) - \chi_i(\tilde{\omega}_n) \tilde{\Delta}_i(i\omega_n)], \quad (28)$$

$$\tilde{\Delta}_i(i\omega_n) = \pi T \sum_m [\lambda(\omega_n - \omega_m) - \mu^*] \times [\chi_r(\tilde{\omega}_m) \tilde{\Delta}_i(i\omega_m) + \chi_i(\tilde{\omega}_m) \tilde{\Delta}_r(i\omega_m)] + \pi t_+ [\chi_r(\tilde{\omega}_n) \tilde{\Delta}_i(i\omega_n) + \chi_i(\tilde{\omega}_n) \tilde{\Delta}_r(i\omega_n)], \quad (29)$$

which, together with Eq. (14a), completely define the electron Green's function of the superconducting alloy. The parameter α , for which the system of equations (14a), (28), and (29) has nontrivial solutions for $\tilde{\Delta}_r$ and $\tilde{\Delta}_i$, defines the upper critical magnetic field according to Eq. (25).

It is interesting to note that the imaginary part of the gap function $\tilde{\Delta}_i$ can be interpreted—according to Fenton and Psaltakis²⁷—as the gap function of triplet Cooper pairs which are antisymmetric in time. Thus, Pauli limiting leads to the interesting physical behavior of triplet pairing even in conventional superconductors. If we use

all the symmetries connected with the functions involved in Eq. (29), we furthermore see that the part connected to the Coulomb pseudopotential μ^* cancels in summing over the m , with the result that the influence of the Coulomb interaction influences the triplet pairs only via the gap function $\tilde{\Delta}_r$ of the standard singlet pairs.

If we neglect Pauli limiting, Eqs. (14a), (28), and (29) reduce to a form already reported by Schachinger *et al.*:^{21,22}

$$\tilde{\Delta}_n(i\omega_n) = \pi T \sum_m \frac{[\lambda(\omega_n - \omega_m) - \mu^*] \tilde{\Delta}_m(i\omega_m)}{\chi^{-1}(\tilde{\omega}_m) - \pi t_+}, \quad (30)$$

$$\tilde{\omega}_n = \omega_n + \pi T \sum_m \lambda(\omega_n - \omega_m) \operatorname{sgn}(\tilde{\omega}_m) + \pi t_+ \operatorname{sgn}(\tilde{\omega}_n), \quad (31)$$

with

$$\chi(\tilde{\omega}_n) = \frac{2}{\sqrt{\alpha}} \int_0^\infty dq \exp(-q^2) \tan^{-1} [q(\alpha/|\tilde{\omega}_n|)^{1/2}]. \quad (32)$$

It was also shown in this paper that Eqs. (30)–(32) reduce to the “dirty-limit” equations (t_+ to ∞) used by Rainer and Bergman¹³ to calculate functional derivatives of H_{c2} . If we furthermore introduce the two-square-well model for the $\lambda(\omega_n - \omega_m)$, i.e., use the approximation²⁸

$$\lambda(\omega_n - \omega_m) = \lambda(0) \Theta(\omega_c - \omega_n) \Theta(\omega_c - \omega_m), \quad (33)$$

with $\Theta(x)$ the step function, Eqs. (30)–(32) reduce to the results of the WHH theory, with $\chi^{-1}(\tilde{\omega}_n)$ and t_+ renormalized by a factor of $1/[1 + \lambda(0)]$. $\lambda(0)$ is the mass-rehancement factor in the BCS limit of the strong-coupling theory. Finally, if we introduce the renormalized Fermi velocity $v_F^* = v_F[1 + \lambda(0)]$, we arrive at the WHH theory formulas as they were quoted by Decroux and Fischer²⁹ and as they were used by Orlando *et al.*¹⁶

In closing we want to remark that in the “clean limit” ($t_+ = 0$) the WHH theory in their $1 + \lambda(0)$ renormalized version shows no $\lambda(0)$ dependency at all, because all the $1 + \lambda(0)$ terms cancel. This implies that, at least in the clean limit, there should be no dependency on strong-coupling parameters.

III. NUMERICAL RESULTS

A. Niobium

In a first step we investigate how strong-coupling effects the theoretical predictions for the transition-metal niobium and we compare the results of our calculations to experimental data. The material niobium is of special interest because there are three different sets of $\alpha^2 F(\Omega)$ spectra available³⁰ and the system was recently investigated experimentally very thoroughly by Laa *et al.*^{31,32} in its impurity dependence.

As H_{c2} of niobium is of the order of 3–5 T, we can restrict our study to Eqs. (30)–(32) because there is no need to include Pauli paramagnetic limiting (PPL) to this calculation. Furthermore, the different sets of $\alpha^2 F(\Omega)$ spectra allow one to investigate how, if at all, the spectrum in-

fluences the predictions of the theory. Figure 1 presents the spectra; spectrum I (dotted line) was calculated by Butler *et al.*³³ from band-structure calculations, spectrum II (dashed line) was measured by Arnold *et al.*,³⁴ and finally spectrum III (solid line) was reported by Robinson and Rowell.³⁵ We see that the spectra differ substantially from each other. The mass-enhancement factor and the Coulomb potential μ^* are for a $T_c = 9.112$ K and a cutoff frequency of $\omega_c = 6\omega_D = 171$ meV (ω_D is the Debye frequency): 1.11 and 0.33 for spectrum I, 1.0 and 0.175 for spectrum II, and 0.983 and 0.113 for spectrum III. (The Nb sample with a nitrogen content of 0.3 at. % and a T_c of 9.112 K was chosen because the impurity data of Laa *et al.*³¹ indicated that this sample had an almost isotropic electron-phonon interaction.)

Figure 2 presents the reduced upper critical magnetic field $h_{c2} = |H_{c2}/[(dH_{c2}/dT)|_{T_c} T_c]|$ in the clean limit ($t_+ = 0$) as a function of the reduced temperature $t = T/T_c$ for the three spectra under consideration. In the region $0.4 \leq t \leq 1.0$ the deviations of the three different results are within plotting accuracy, but at lower temperatures the three curves start to deviate from each other (see inset 1), with the largest difference at $t = 0$. We see that spectrum III with the largest weight in $\alpha^2 F(\Omega)$ in the region $0 \leq \Omega \leq 8.0$ meV also gives the largest $h_{c2}(0)$. This result is in agreement with the dirty-limit results for the functional derivative $\delta h_{c2}(0)/\delta \alpha^2 F(\Omega)$ by Rainer and Bergman (Fig. 10 of Ref. 13), from which we find that the most important frequencies for $h_{c2}(0)$ are in the region $4 \leq \Omega \leq 8$ meV, with a maximum at about 6 meV. Thus it is the specific shape of the spectrum in this region which actually determines the low-temperature behavior rather than the value of the mass-enhancement factor λ , which is often regarded as a measure of the low-frequency weight in $\alpha^2 F(\Omega)$. [A similar result for $h_{c2}(t)$ was already reported in the theoretical study by Schachinger *et al.*^{21,22} for the case of $\text{Cu}_2\text{Mo}_6\text{Se}_8$.] The calculations clearly prove that in contrast to the BCS-type WHH theory, a strong-coupling theory shows a distinctive influence of the shape of the electron-phonon-interaction spectral

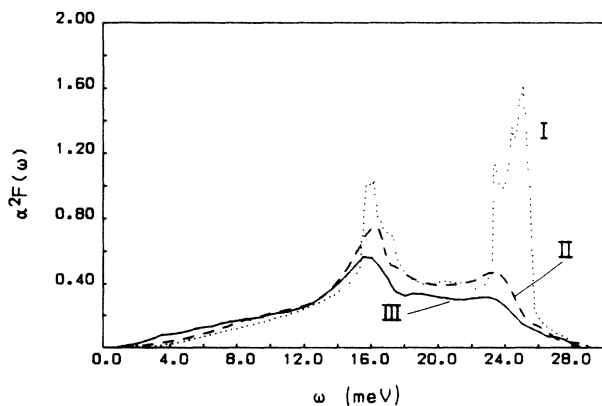


FIG. 1. $\alpha^2 F(\Omega)$ spectrum for niobium as it is reported by Butler *et al.* (Ref. 33) (dotted line, "spectrum I"), by Arnold *et al.* (Ref. 34) (dashed line, "spectrum II"), and by Robinson and Rowell (Ref. 35) (solid line, "spectrum III").

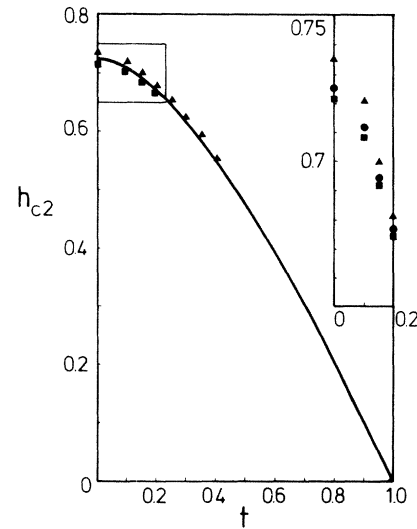


FIG. 2. Reduced critical field $h_{c2} = H_{c2}/[(dH_{c2}/dT)T_c]$ as a function of the reduced temperature $t = T/T_c$. The solid line connects the results for spectrum II. Spectrum I is presented by solid squares, spectrum II by solid circles, and spectrum III by solid triangles.

function on the upper critical field. This point becomes even more transparent in Fig. 3, where the parameter $\alpha(t)$ which is proportional to H_{c2}/v_F^2 is plotted versus the reduced temperature t . Spectrum III gives the largest values for $\alpha(t)$ and spectrum I the smallest ones, with the consequence that the Fermi velocity has to be larger in case of spectrum III in order to give the same experimental H_{c2} at a given temperature as for instance for spectrum I.

Unfortunately, in deriving $\alpha^2 F(\Omega)$ data from tunneling

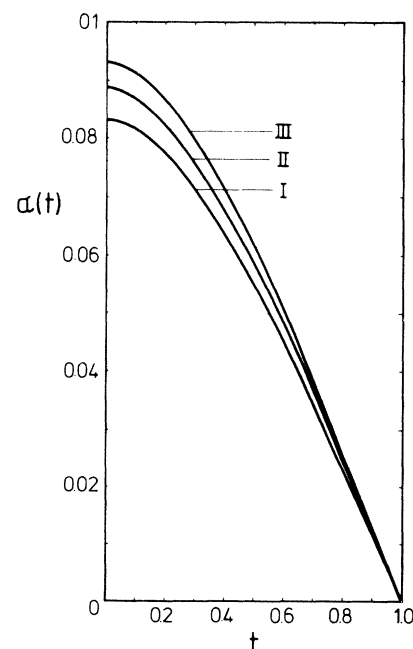


FIG. 3. Eigenvalue $\alpha(t)$ in 10^{12} T/(m²/s²) as a function of the reduced temperature for the three spectra of Fig. 1.

experiments a quadratic fit is performed in the low-frequency range, the range which is important for the size of $h_{c2}(0)$. Thus, fitting theoretical $h_{c2}(t)$ data to the experiment will not result in a clear answer to the question of which of the three spectra is the “correct” one, but it will give a tool with which to perform this quadratic fit more accurately in future inversions of tunneling data.

Thus it is rather a question of personal taste that we finally fit the theory to the experimental $H_{c2}(T)$ data³² for the polycrystalline Nb sample with 0.3 at. % nitrogen using spectrum III. The sample cannot be regarded as clean and therefore we have to fit the transport relaxation-time parameter t_+ and the Fermi velocity v_F . As v_F enters Eqs. (30)–(32) only via α and not explicitly, it is obvious that the reduced critical field is only a function of t_+ and can be calculated as $|\alpha(T)/[d\alpha(T)/dT|_{T_c} T_c]|$. Therefore t_+ is to be fitted to give one of the experimental values and we chose the point $T=5.0$ K with a $B_{c2}=283.2\pm 0.94$ mT, which results in an h_{c2} of 0.427 ± 0.0014 . The theory reproduces this result for a $t_+=0.76$ meV and this fit is already sufficient to reproduce the experimental $h_{c2}(t)$ over the whole temperature range. (If this were not the case, the quantum-mechanical model would have been incomplete.) v_F plays only the role of a factor of proportionality and can be fitted to any one of the actual B_{c2} values. We find $v_F=0.486\times 10^6$ m/s, and Fig. 4 proves that the theory fits the experiment

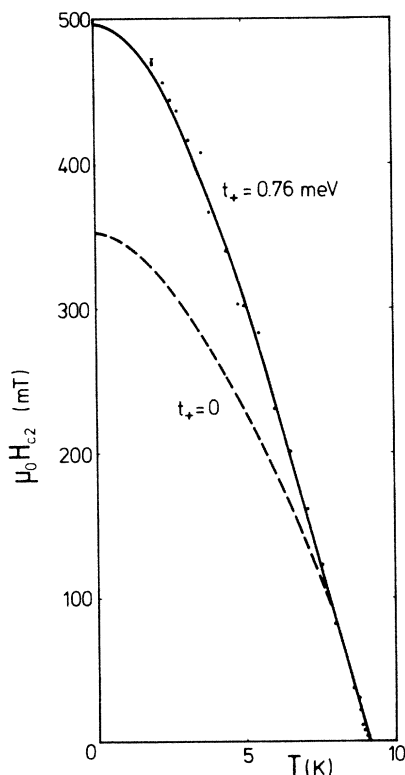


FIG. 4. Results of a full strong-coupling calculation for the niobium polycrystal with 0.3 at. % nitrogen. The solid line represents the results for a $t_+=0.76$ meV and for a Fermi velocity $v_F=0.468\times 10^6$ m/s. The dashed line gives the result for the “clean” limit. The solid circles represent the experimental data by Laa (Ref. 32). (The experimental error is about 0.35%.)

almost perfectly. (If we use one of the other spectra we will find somewhat different values for t_+ and v_F , and the agreement between theory and experiment is not quite as good in the low-temperature region $t < 0.35$.) A close examination of Fig. 4 reveals that there is a systematic deviation of the experiment from the theory close to T_c and at low temperatures. We believe that these deviations are due to the remaining anisotropy in the sample, as one can clearly see from the T_c -versus-impurity curve shown in Ref. 31 and from the results reported by Seidl *et al.*³⁶ This may also account for the rather small value of t_+ necessary to get a proper fit. The Fermi velocity found is in very good agreement with the average Fermi velocity for niobium reported by Crabtree *et al.*³⁷

In conclusion, we can state that even for the rather weak-coupling material niobium, a strong-coupling analysis of the experimental data is essential to achieve agreement between theory and experiment over the whole temperature range. It is not necessary to include PPL, and spin-orbit scattering is of no importance at all.

B. The A15 compound V₃Si

The experimental results reported by Foner and McNiff²³ for a V₃Si single crystal with a T_c of 16.4 K and a residual resistivity ρ_0 of 52 nΩm were already analyzed by Orlando *et al.*¹⁶ using a strong-coupling renormalized WHH theory. They found that in order to explain the experimental data, PPL as well as substantial spin-orbit scattering had to be included in order to reproduce the data in a satisfactory way.

In the meanwhile, $\alpha^2 F(\Omega)$ data were derived by Kihlstrom³⁸ from tunneling experiments, by McKnight *et al.*³⁹ from far-infrared-absorption experiments, and the generalized phonon density of states $G(\Omega)$ was found by inelastic-neutron-scattering experiments.⁴⁰ It was shown by Mitrović and Carbotte⁴¹ that $\alpha^2 F(\Omega)$ data found by rescaling the $G(\Omega)$ data by a constant factor to give a λ of 1 was sufficient to achieve a reasonable agreement between the results of a strong-coupling calculation and thermodynamics data found by experiment. It was also shown by these authors that the far-infrared-absorption-derived data lead to a less satisfying agreement with the thermodynamics data of V₃Si. Very recently, Kihlstrom demonstrated in his paper that the $\alpha^2 F(\Omega)$ of V₃Si does not show a “phonon softening” as the samples approach stoichiometry, as was reported for other A15 compounds; the weight is simply increased for all frequencies. Thus it seems to be of interest to compare the results of a strong-coupling H_{c2} calculation using the rescaled $G(\Omega)$ with $\lambda=1.0$ and the $\alpha^2 F(\Omega)$ data found by Kihlstrom for his sample 3 ($T_c=15.4$ K, $\lambda=0.89$) rescaled to give a λ of 1.0. The resulting spectra are compared in Fig. 5 and one immediately recognizes that the spectrum by Kihlstrom (solid line, spectrum I) shows less weight at low frequencies than the rescaled $G(\Omega)$ distribution (dotted line, spectrum II).

We have to include PPL and therefore the complete set of Eqs. (14a), (28), and (29) has to be solved simultaneously. In a first step the results for the two spectra are compared in the clean limit for $T=0$ K. ($T_c=16.4$ K in both

cases; $\omega_c = 6\omega_D = 267$ meV, giving a μ^* of 0.136 for spectrum I and of 0.152 for spectrum II.) For the reduced upper critical field $h_{c2}(0)$ without PPL we find 0.7255 for spectrum I and 0.7267 for spectrum II as a result of the slight differences in the spectra at low frequencies. (A WHH calculation would give, for $h_{c2}(0)$, 0.69.¹⁶) If we include PPL the reduced field h_{c2} is suppressed substantially at low temperatures resulting in a $h_{c2}(0)$ of 0.665 for both spectra. Thus it is no longer of any importance which of the two spectra is actually used because a small gain in h_{c2} is immediately suppressed by a more effective PPL.

We decided to use spectrum I for further calculations. Again we have to fit the “free” parameters t_+ and v_F to the experiment. In contrast to the Nb case, it is now no longer possible to decouple the effects of t_+ and v_F because of Eq. (24). Nevertheless, it is possible to fit the two parameters quite independently, keeping in mind that close to T_c PPL is not effective and the theory without PPL [Eqs. (30)–(32)] can be applied. Thus we fit t_+ to give one of the high-temperature h_{c2} values and then in a second step we have to fit v_F to reproduce the whole $h_{c2}(T)$ curve using the full theory. Having established both parameters, the theory has to reproduce the $H_{c2}(T)$ curve correctly.

Figure 6 presents the results of such a calculation. The open squares in this figure correspond to the experimental data,^{16,23} which were read off Fig. 8 of Ref. 16 and Fig. 1 of Ref. 23. The solid curves correspond to the results of the strong-coupling calculations including PPL. We see that with a $t_+ = 5.1$ meV and a Fermi-surface velocity of $v_F = 0.168 \times 10^6$ m/s the experimental data are reproduced perfectly. This v_F value is in excellent agreement with data found by Klein *et al.*⁴² from band-structure calculations ($\langle v_F \rangle = 0.172 \times 10^6$ m/s). In order to emphasize the effect of the PPL we also include the results of a strong-coupling calculation without PPL (dashed lines). The effect of the transport relaxation time on H_{c2} becomes

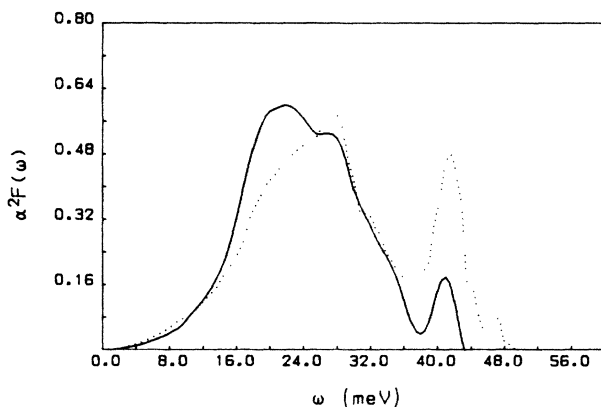


FIG. 5. $\alpha^2 F(\Omega)$ spectrum for V_3Si . The dotted line corresponds to the generalized phonon density of states $G(\Omega)$ as it was measured by Schweiss *et al.* (Ref. 40); the solid line represents the $\alpha^2 F(\Omega)$ spectrum as it was measured by Kihlstrom (Ref. 38). Both spectra are renormalized to give a mass-enhancement factor of 1.0.

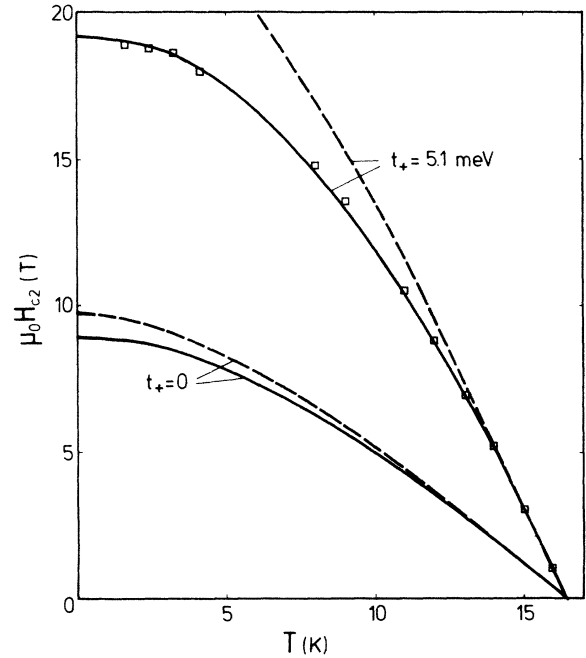


FIG. 6. Comparison theory—experiment for V_3Si . The open squares correspond to the data for the V_3Si single crystal reported by Foner and McNiff (Ref. 23). (Some errors may arise from the fact that we had to read the data off the graphs in Refs. 16 and 23.) The solid line represents the results of our calculation for a $t_+ = 5.1$ meV and a Fermi velocity of $v_F = 0.168 \times 10^6$ m/s. The results of a calculation without Pauli spin paramagnetism (dashed lines) and for the “clean” limit are included for comparison.

transparent from comparison to clean-limit results ($t_+ = 0$).

If we take the electronic density of states at the Fermi level, $N(0) = 13.64 \times 10^{19}$ states/meV cm^3 spin,⁴¹ and the above Fermi velocity, the Drude plasma frequency becomes $\hbar\Omega_d = 7.484$ eV. This gives, together with the above value of t_+ , residual resistivity of $\rho_0 = 42.5$ n Ω m, which is in excellent agreement with the experimental value of ρ_0 concerning the still substantial uncertainties in determining the proper $N(0)$ value of V_3Si .⁴¹

In closing, it is necessary to emphasize that this calculation does not include spin-orbit-scattering contributions; they are obviously not necessary to explain the experiment. The effect of such contributions in the WHH theory is that the H_{c2} values calculated at low temperatures are enhanced. This is necessary as the BCS-related theories usually result in intolerable deviations to smaller H_{c2} values at low temperatures, while the high-temperature region is explained by these theories in a quite satisfying way. From the above calculations, it becomes transparent that it is the impurity scattering in the clean limit and the electron-phonon—interaction effects, together with a strong Pauli paramagnetic limiting, which govern the temperature dependence of H_{c2} in V_3Si .

IV. CONCLUSION

In this paper we presented for the first time full strong-coupling equations on the imaginary axis for the

upper critical magnetic field H_{c2} which are valid over the whole temperature range. These equations include the effect of momentum scattering of the conduction electrons at randomly distributed impurity sites and the effect of the Pauli spin paramagnetism. The equations do not include the effect of spin-orbit scattering. It was found that the Pauli spin paramagnetism results in a complex gap function, where the real part could be interpreted as the standard gap function related to singlet Cooper pairs, while the imaginary part was interpreted as a gap function which is related to triplet Cooper pairs antisymmetric in time.

The results of numerical calculations were tested against experimental data reported for an almost isotropic polycrystalline niobium sample and the data found for a V_3Si single crystal. In the first case we find good agreement between theory and experiment, except for some minor deviations at low temperatures and at temperatures very close to the critical one which we believe are related to a remaining anisotropy of the sample. It was not necessary to include PPL in order to explain the experimental data.

It becomes necessary to include PPL in the case of V_3Si . In this regard we agree completely with the analysis of Orlando *et al.*,¹⁶ but in contrast to their results we do

not have to include spin-orbit scattering, and the value found for the Fermi velocity is larger and in better agreement with the results of band-structure calculations.

It is the main result of this study that the strong-coupling correction results in larger values for H_{c2} in the low-temperature regime compared to the results one would achieve by BCS-related calculations. This increase in H_{c2} is sufficient to explain the experiment even in this regime (except eventual anisotropy effects) and we conclude that in most cases where it was necessary to include spin-orbit scattering in order to fit theory to experiment this contribution was only a substitute for the strong-coupling effects apparent in this temperature regime. We also found that the low-frequency part of the $\alpha^2F(\Omega)$ spectrum mainly controls the low-temperature behavior of H_{c2} , but this result is open to more rigorous proof by calculating the functional derivatives of $h_{c2}(0)$ with respect to changes in $\alpha^2F(\Omega)$, which will become our next task.

ACKNOWLEDGMENTS

The authors are very grateful to Dr. H. W. Weber and Dr. K. E. Kihlstrom for providing their experimental data prior to publication.

- ¹V. L. Ginzburg and L. D. Landau, *Zh. Eksp. Teor. Fiz.* **20**, 1064 (1950).
- ²A. A. Abrikosov, *Zh. Eksp. Teor. Fiz.* **32**, 1442 (1957) [*Sov. Phys.—JETP* **5**, 1174 (1957)].
- ³L. P. Gor'kov, *Zh. Eksp. Teor. Fiz.* **36**, 1918 (1959) [*Sov. Phys.—JETP* **9**, 1364 (1959)]; **37**, 1407 (1959) [**10**, 998 (1960)].
- ⁴K. Maki, *Physics* **1**, 21 (1964).
- ⁵P. G. de Gennes, *Phys. Kondens. Mater.* **3**, 79 (1964).
- ⁶E. Helfand and N. R. Werthamer, *Phys. Rev. Lett.* **13**, 686 (1964).
- ⁷E. Helfand and N. R. Werthamer, *Phys. Rev.* **147**, 288 (1966).
- ⁸N. R. Werthamer, E. Helfand, and P. C. Hohenberg, *Phys. Rev.* **147**, 295 (1966).
- ⁹N. R. Werthamer and W. L. McMillan, *Phys. Rev.* **158**, 415 (1967).
- ¹⁰G. M. Eliashberg, *Zh. Eksp. Teor. Fiz.* **38**, 966 (1960) [*Sov. Phys.—JETP* **11**, 696 (1960)].
- ¹¹G. Eilenberger and V. Ambegaokar, *Phys. Rev.* **158**, 332 (1967).
- ¹²K. D. Usadel, *Phys. Rev. B* **2**, 135 (1970).
- ¹³D. Rainer and G. Bergmann, *J. Low Temp. Phys.* **14**, 501 (1974).
- ¹⁴D. Rainer, G. Bergmann, and U. Eckhardt, *Phys. Rev. B* **8**, 5324 (1973).
- ¹⁵M. Schossmann and E. Schachinger, *Phys. Rev. B* **30**, 1349 (1984).
- ¹⁶T. P. Orlando, E. J. McNiff, Jr., S. Foner, and M. R. Beasley, *Phys. Rev. B* **19**, 4545 (1979).
- ¹⁷E. Schachinger, J. M. Daams, and J. P. Carbotte, *Phys. Rev. B* **22**, 3194 (1980).
- ¹⁸E. Schachinger and J. P. Carbotte, *Phys. Rev. B* **29**, 165 (1984).
- ¹⁹E. Schachinger and R. Wunder, *Physica* **135B**, 464 (1985).
- ²⁰M. Schossmann, Ph.D. thesis, Technical University of Graz, 1984 (unpublished).
- ²¹E. Schachinger, H. G. Zarate, M. Schossmann, and J. P. Carbotte, *Physica* **135B**, 377 (1985).
- ²²E. Schachinger, H. G. Zarate, M. Schossmann, and J. P. Carbotte, *J. Low. Temp. Phys.* (to be published).
- ²³S. Foner and E. J. McNiff, Jr., *Appl. Phys. Lett.* **32**, 122 (1978).
- ²⁴Y. Nambu, *Phys. Rev.* **117**, 648 (1960).
- ²⁵A. A. Abrikosov and L. P. Gor'kov, *Zh. Eksp. Teor. Fiz.* **39**, 1781 (1960) [*Sov. Phys.—JETP* **12**, 1243 (1961)].
- ²⁶J. Bardeen and M. Stephen, *Phys. Rev.* **136**, A1485 (1964).
- ²⁷E. W. Fenton and G. C. Psaltakis, in *Superconductivity in d- and f-Band Metals*, edited by W. Buckel and W. Weber (Kernforschungszentrum Karlsruhe, Karlsruhe, 1982), p. 531.
- ²⁸P. B. Allen and B. Mitrović, in *Solid State Physics*, edited by H. Ehrenreich, F. Seitz, and D. Turnbull (Academic, New York, 1982), Vol. 37, p. 1.
- ²⁹M. Decroux and Ø. Fischer, in *Superconductivity in Ternary Compounds II*, edited by M. B. Maple and Ø. Fischer (Springer-Verlag, Berlin, 1982), p. 57.
- ³⁰W. H. Butler, in *Superconductivity in d- and f-Band Metals*, edited by H. Suhl and M. B. Maple (Academic, New York, 1980), p. 443.
- ³¹C. Laa, E. Seidel, and H. W. Weber, in *LT-17 (Contributed Papers)*, edited by U. Eckern, A. Schmid, W. Weber, and H. Wühl (Elsevier, New York, 1984), p. 1283.
- ³²C. Laa, Master's thesis, Technische Universität Wien, 1984 (unpublished).
- ³³W. H. Butler, F. J. Pinski, and P. B. Allen, *Phys. Rev. B* **19**, 3708 (1979).
- ³⁴G. B. Arnold, J. Zasadzinski, J. W. Osmun, and E. L. Wolf, *J. Low Temp. Phys.* **40**, 225 (1980).
- ³⁵B. Robinson and J. M. Rowell, in *Proceedings of the International Conference on the Physics of Transition Metals, Toronto*

- to*, 1977, edited by M. J. G. Lee, J. M. Perz, and E. Fawcett (IOP, London, 1978), p. 666.
- ³⁶E. Seidel, H. W. Weber, and H. Teichler, *J. Low Temp. Phys.* **30**, 273 (1978).
- ³⁷G. W. Crabtree, D. H. Dye, D. P. Karim, D. D. Koelling, and J. P. Ketterson, *Phys. Rev. Lett.* **42**, 390 (1979).
- ³⁸K. E. Kihlstrom, *Phys. Rev. B* **32**, 2891 (1985), and private communication.
- ³⁹S. W. McKnight, S. Perkowitz, D. B. Tanner, and L. R. Testardi, *Phys. Rev. B* **19**, 5689 (1979).
- ⁴⁰B. P. Schweiss, B. Renker, E. Schneider, and W. Reichardt, in *Superconductivity in d- and f-Band Metals*, edited by D. H. Douglass (Plenum, New York, 1976).
- ⁴¹B. Mitrović and J. P. Carbotte, *Phys. Rev. B* **26**, 1244 (1982).
- ⁴²B. M. Klein, D. A. Papaconstantopoulos, and L. L. Boyer, in *Superconductivity in d- and f-Band Metals*, Ref. 30, 455.